INORGANIC CHEMISTRY FRONTIERS

CHINESE CHEMICAL SOCIETY | ROYAL SOCIETY OF CHEMISTRY

RESEARCH ARTICLE

View Article Online
View Journal | View Issue

Check for updates

Cite this: *Inorg. Chem. Front.*, 2021, **8**, 4415

In situ determination of the interplay of the structure and domain under a subcoercive field in $BiScO_3–PbTiO_3$†

Longlong Fan, *[a,b] Linxing Zhang, [c] Hui Liu,[d] Yu-sheng Chen,[b] Yang Ren,[e] Xianran Xing [f] and Jun Chen [d,f]

Received 26th May 2021,
Accepted 30th July 2021

DOI: 10.1039/d1qi00670c

rsc.li/frontiers-inorganic

The extraordinary performances of phase-coexisting ferroelectrics are significantly affected by not only the phase constitution but also the motion of domain walls. The study on the role of phase coexistence in the formation of ferroelectric and ferroelastic domain microstructures is of great importance to explain the enhanced piezoelectric properties. *In situ* high-energy diffraction and the Rayleigh law are utilized to reveal the interplay of phase constitution and domain configuration to the macroscopic electromechanical coupling effect in the morphotropic phase boundary composition of $0.365BiScO_3–0.635PbTiO_3$ during the application of a weak electrical loading in the present study. It was found that anisotropic phase transition and domain switching occur in polycrystalline ferroelectric ceramics and a phase transition occurs dramatically beyond the coercive field. Taking into account the important role of coupled ferroelectric and ferroelastic domain microstructures, we conceived a configuration of monoclinic domains coexisting with and bridging the tetragonal domains. The existence of bridging domains would provide an insight into the interplay of the phase and domain and explains the piezoelectric performance in the vicinity of morphotropic phase boundaries.

Introduction

In piezoelectric materials, the motion of domain walls is known to significantly affect their dielectric, piezoelectric, and ferroelectric properties. Understanding not only the ferroelectric domain but also the ferroelectric domain boundary becomes more essential for the development of piezoelectric materials and devices. For example, investigations demonstrated that the formation of nanodomains assists ferroelastic domain switching and reduces the threshold field for domain propagation.[1] The movement of ferroelastic domain walls significantly enhanced the piezoelectric coefficient of a ferroelectric thin film.[2] A significant reduction of the stiffness at the domain boundary promoted the switching of domains to enhance the piezoelectric properties.[3] The pinning of the ferroelectric domain boundary motion induced the polarization fatigue in the ferroelectric thin film.[4]

Thermodynamically, the phase coexistence in ferroelectric compounds accessing the morphotropic phase boundary (MPB) regions also improves the dielectric and piezoelectric properties and electromechanical coupling.[5–7] The MPB of a solid solution separates the phase components possessing an approximate energetic landscape with different orientations of polarization. The flattened free energy around the MPB benefits the field-driven phase transformation, facilitating the rearrangement of polar in domains under an electric field as reported for PZT,[7,8] $PbTiO_3–BiScO_3$,[9,10] *etc.* Meanwhile, a strong synergy between the reversible phase transition and enhanced domain switching exists near MPBs and plays an important role in improving the piezoelectric responses.[10,11] These studies provide a broad aspect of the MPB phase coexistence phenomenon. Since investigations including transmission electron microscopy (TEM) have revealed that the existence of mottled nanometer ferroelectric domains for the MPB composition would be highly related to the phase compo-

[a] *College of Physics and Materials Science, Tianjin Normal University, Tianjin 300387, China. E-mail: longl.fan@gmail.com*
[b] *NSF's ChemMatCARS Beamline@APS, The University of Chicago, Argonne, IL, 60439, USA*
[c] *Institute for Advanced Materials and Technology, University of Science and Technology Beijing, Beijing 100083, China*
[d] *School of Mathematics and Physics, University of Science and Technology Beijing, Beijing 100083, China*
[e] *X-Ray Science Division, Advanced Photon Source, Argonne National Laboratory, Argonne, Illinois 60439, USA*
[f] *Beijing Advanced Innovation Center for Materials Genome Engineering, Institute of Solid State Chemistry, University of Science and Technology Beijing, Beijing 100083, China*

†Electronic supplementary information (ESI) available. See DOI: 10.1039/d1qi00670c

sition and be the crucial factor responsible for the excellent piezoelectric response,[12,13] the role of phase coexistence in the change of ferroelectric and ferroelastic domain microstructures must be considered in order to account for the enhanced piezoelectric properties.

Experimentally, X-ray and neutron Bragg scattering techniques would be versatile tools to be utilized to quantitatively investigate ferroelastic domain wall motion and phase transition in polycrystalline materials because, crystallographically, the lattice deformation and average displacement of domain walls can be tracked by the changes in the peak position and crystallographic texture observed during the loading process.[14] Hence, *in situ* X-ray diffraction combined with two-dimensional (2D) scattering geometry technology would be helpful to construct a comprehensive picture of structural evolution and domain switching behavior, and the information of phase transition, intrinsic effects (including polarization vector rotation and lattice distortion under an external stimulus), and extrinsic effects (mainly including domain wall motion) can also be simultaneously extracted to elaborate their contributions to the piezoelectric behavior. Because Pb/Bi-based perovskites exhibit an extremely high T_C value and large piezoelectricity and in some cases multiferroic behavior, binary systems of $PbTiO_3$–$BiMeO_3$ have been intensely researched. In the present study, a high-T_C and high performance MPB piezoceramic material with a composition of $0.365BiScO_3$–$0.635PbTiO_3$ (0.365BS–0.635PT) was employed to investigate the role of phase coexistence in the domain wall motion. To assess the total influence of the domain wall and interphase boundary motion on the piezoelectric behaviors, the Rayleigh law in association with *in situ* high-energy diffraction was used. Based on the fact that the relative nonlinear contributions in the Rayleigh coefficient originate from the displacements of ferroelectric domain walls and/or the phase boundary, the changes in the converse piezoelectric coefficient and *in situ* diffraction profiles convince that a phase transition occurs dramatically beyond the coercive field. A landscape of the tetragonal domains bridged by the monoclinic phase or domains has been constructed to elaborate the piezoelectric performance. It is suggested that a transition area would exist between the domains of the tetragonal and monoclinic phases, and the transition area plays a pivotal role in the piezoelectric performance.

Experimental section

A solid-state reaction method was used to prepare the samples of 0.365BS–0.635PT. Analytically pure starting powders of PbO, Bi_2O_3, TiO_2, and Sc_2O_3 were stoichiometrically mixed and milled in a mortar with ethanol for 2 h. After drying, the mixture was calcined at 750 °C for 4 h, and the obtained green ceramic pellets were sintered at 1125 °C for 2 hours in a closed crucible covered with a sacrificial powder. Then, the powder XRD pattern of the ground ceramic powder confirmed the phase purity and coexistence of the tetragonal and monoclinic phases at the MPB as stated in prior observations.[15–17] The pellets were polished on abrasive paper, and gold electrodes were deposited on the top and bottom surfaces. Polarization and strain loops of the 0.36BS–0.64PT ceramic were characterized on initially unpoled materials using a ferroelectric analyzer at various field amplitudes and frequencies (TF Analyzer 1000, aixACCT). The piezoelectric parameter was measured using a Berlincourt d_{33} meter (ZJ-3, China Academy of Acoustics, China) after the samples were poled at an electrical loading as high as 7 kV mm^{-1}. The measurements of strain responses of the poled samples were repeated under bipolar field amplitudes varying below and near the coercive field.

In situ high-energy synchrotron XRD (HEXRD) investigations using a wavelength of 0.11165 Å were performed on the beamline 11-ID-C at the Advanced Photon Source, Argonne National Laboratory. The beam size incident on the material was 0.5 mm × 0.5 mm. The samples for *in situ* experiments were prepared by cutting into dimensions of 1 mm × 1.2 mm × 5 mm. The electric field was applied perpendicular to the beam direction using a high voltage amplifier. Diffraction patterns were obtained in a forward scattering geometry (transmission mode) on a PerkinElmer amorphous silicon area detector placed at approximately 1600 mm from the sample stage. The high energy X-ray penetrated the thick Pb/Bi-based ceramics and was adapted for the investigation of the bulk response under an external electric field.

To determine the evolution of the phase structure as a function of the electric field, a triangular step shaped waveform with an amplitude of 6 kV mm^{-1} and a step size of 0.5 kV mm^{-1} was applied. A relatively longer duration (about 60 s) for data collection was used to collect high-quality diffraction data for reliable structure determination. Hence, the bipolar cycling frequency was about 0.33 mHz. During the diffraction analysis, the Debye rings under different electric fields were divided into different azimuthal sectors at an interval of 15° to integrate the diffraction intensities. Considering the symmetric nature of the diffraction data, only the first quadrant, $0 \le \varphi \le \pi/2$, of the data is presented in this work. The diffraction patterns collected at the 0° sector, which is parallel to the direction of the electric field, are utilized to extract the domain volume and lattice deformation under the electrical stimulus. According to our previous investigation, the diffraction data obtained at the 45° sector are utilized for crystal structure analysis. The structural refinements were performed using the FULLPROF program.

Results and discussion

The ferroelectric compounds of $BiScO_3$–$PbTiO_3$ at the MPB have been widely studied owing to their known excellent properties. Herein, the piezoelectric and ferroelectric properties of 0.365BS–0.635PT were quantitatively measured, and the direct piezoelectric coefficient was calculated to be about 440 pC N^{-1}. The coercive field (E_c) has been determined to be about 2.7 kV mm^{-1} from the polarization and strain measurements in response to bipolar electric field amplitudes at ±7 kV mm^{-1} and a frequency of 1 Hz (Fig. S1†). The maximum and remanent polarization reached up to 49 and 38 μC cm^{-2}, respectively, and the peak-to-peak strain recorded was 0.55%. After poling under 7 kV mm^{-1}, the piezoelectric coefficient was obtained as a function of the frequency of ac electrical loading, at an ac electrical loading of ~1 kV mm^{-1}. The maximum strain values obtained in the positive and negative field directions were used to calculate the converse piezoelectric coefficient as a function of frequencies ranging from 0.5 to 100 Hz. The results are shown in Fig. 1a and b. The piezoelectric coefficient decreases monotonically with the logarithm of the frequency and could be well represented with the linear equation, $d_{33}(\omega) = d_0 + \beta \ln(1/\omega)$, where d_0 and β are 481.7 and 16.4 pm V^{-1}, respectively. Herein, the piezoelectric coefficient obtained using a Berlincourt d_{33} meter is lower than the d_0 value, while it is approximate to the $d_{33}(\omega)$ value at about 10 Hz. The change in the frequency dependent piezoelectric coefficient would be due to the random pinning of the domain walls. Both reversible and irreversible components are frequency dependent in ferroic systems, in which interface pinnings are randomly distributed.[18]

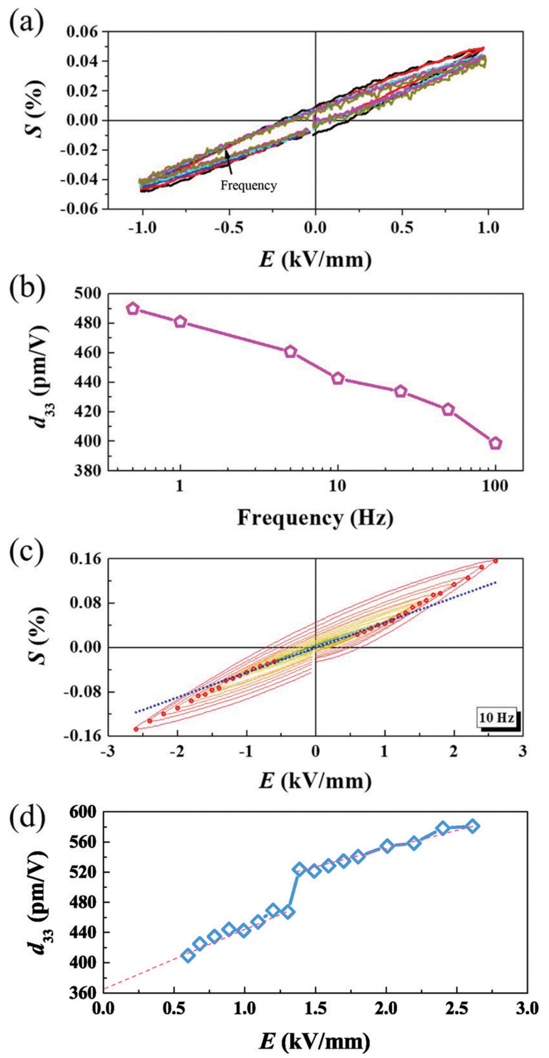

Fig. 1 (a) Strain and (b) piezoelectric coefficient measurements at 1 kV mm^{-1} under various frequencies. (c) Strain and (d) piezoelectric coefficient measurements under a progressively increasing sub-coercive electrical loading of up to 2.6 kV mm^{-1} at 10 Hz. The error in the piezoelectric coefficient is less than 5%.

Then, increasing cyclic electric fields of up to 2.6 kV mm^{-1}, which are in close proximity to the ferroelectric E_c, were progressively applied to the sample in order to study the total influence of the intrinsic and extrinsic effects (including domain wall and interphase boundary motion) on the piezoelectric performance. Fig. 1c and d show the strain measurements and field amplification dependent piezoelectric coefficients. Under a weak field (below $E_c/2 \approx 1.4$ kV mm^{-1}), the field dependent piezoelectric coefficient can be described using a relationship analogous to the Rayleigh law: $d_{33}(E_{max}) = d_{init} + \alpha E_{max}$, where E_{max} is the amplitude of the ac electric field, d_{init} includes reversible contributions such as intrinsic piezoelectric displacement and reversible interface motion, and α represents contributions from the irreversible interface displacements.[19] Herein, the d_{init} and α values are 368.3 pm V^{-1} and 79.7×10^{-18} m^2 V^{-2}, respectively. When measured at a high frequency, both the d_{init} and α values are lower than those reported for 0.36BS–0.64PT.[20,21] Once the electric field exceeds $E_c/2$, a "leap" for the field dependent piezoelectric coefficient is observed. The d_{init} and α values become 446.2 pm V^{-1} and 52.9×10^{-18} m^2 V^{-2}, respectively. Intriguingly, the ratio of α/d_{init} under the weak field is 0.22×10^{-6} m V^{-1}, higher than the value of 0.12×10^{-6} m V^{-1} obtained above $E_c/2$. As the Rayleigh parameters allow for a quantitative determination of the domain wall contributions, a higher α/d_{init} value means that the irreversible contributions are stronger below $E_c/2$ and become weak as the electric field exceeds E_c.[20] To reveal the nature of piezoelectric behaviors, it becomes essential to study the motion of domains and the reconstruction of domain boundaries under *in situ* conditions.

Fig. 2a and b shows the HEXRD patterns in the region of the $\{111\}_{PC}$ and $\{002\}_{PC}$ reflections, where PC refers to the pseudocubic setting during the application of a linear bipolar electric field with the amplitudes being below the E_c. At the $\varphi = 0°$ sector, a change in the average $\{111\}_{PC}$ interplanar spacing is observed, accompanied by significant intensity changes for the $\{002\}_{PC}$ diffraction profile. The changes in the intensities originated from domain switching under the influence of external stimuli.[12,21–23] Between the tetragonal $\{002\}_T(2\theta \approx 3.13)$ and $\{200\}_T(2\theta \approx 3.21)$ reflections, the additional Bragg scattering was suggested to be related to the existence of 002 M and 220 M reflections of a monoclinic phase.[10,24] Due to the overlap of the tetragonal $\{002\}_T$ and $\{200\}_T$ reflections and diffuse scattering, the monoclinic $\{220\}_M$ and $\{002\}_M$ reflections are not easily resolved and considered as a single profile in the following analysis. Under an electrical loading of −1.5 to 2.0 kV mm^{-1}, the diffraction profile of monoclinic phase reflections at the $\varphi = 0°$ sector remains almost unchanged (Fig. 2a), which is discussed in the

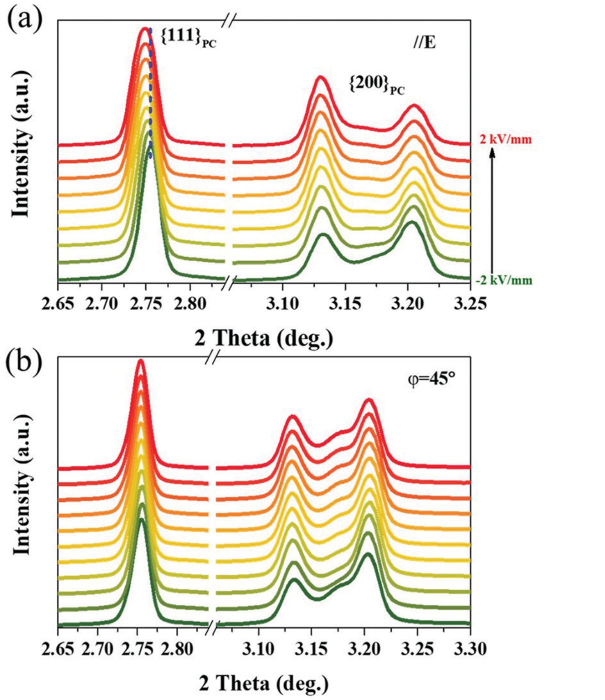

Fig. 2 The diffraction profiles corresponding to the $\{111\}_{PC}$ and $\{200\}_{PC}$ reflections (a) parallel to the electric field and (b) at the φ = 45° sector during the application of a bipolar electric field with amplitudes below the coercive field amplitude (E_c).

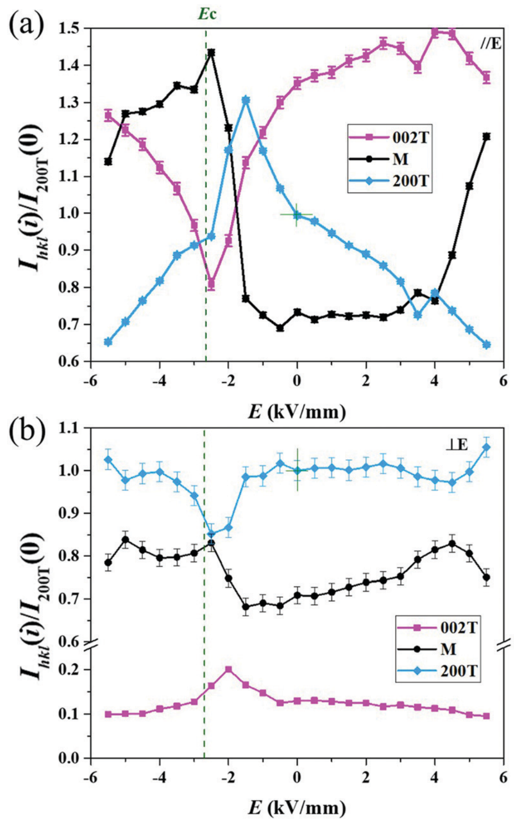

Fig. 3 The evolution of relative intensities of the $\{200\}_{PC}$ reflections (a) parallel and (b) perpendicular to the electric field during the application of a bipolar electric field.

following text, while at the φ = 45° sector both the peak position and relative intensities of the $\{111\}_{PC}$ and $\{002\}_{PC}$ reflections show a slight change upon varying the electrical loading (Fig. 2b). Similar to the results reported in our previous investigation on rhombohedral, tetragonal, and MPB compounds,[8,10,12,25] it is supposed that the diffraction data collected at the φ = 45° sector exclude the influence of the intergranular strain and texture induced by domain switching. The data of the φ = 45° sector were used for structure refinement in the following analysis to evaluate the phase evolution in 0.365BS–0.635PT under an applied electric field.

For piezoelectric ceramics with applied external stimuli, the diffraction intensities of characteristic peaks are mainly susceptible to not only the multiplicity factor but also the structural factor.[24] Considering the structural change of the ferroelectric phase under the electrical loading, it should be more difficult to accurately estimate the variation of the domain volume by the specific peak intensity change. Nevertheless, investigations on the tetragonal phase demonstrate that the $\{h00\}_T$ peaks present both stable structural factors and peak profiles under different electric fields and their intensity change can be utilized for deducing the process of domain motion by evaluating the relative volume change of 001-oriented domains perpendicular to the electric field.[24] Herein, the characteristic reflections of $\{200\}_{PC}$ at φ = 0° and φ = 90° obtained under both the positive and negative electric fields are fitted by three pseudo-Voigt peaks to integrate the intensities of the tetragonal $\{002\}_T$ and$\{200\}_T$ and the reflections from a monoclinic phase. Fig. 3a and b show the changes in their relative intensity to that of the $\{200\}_T$ in the poled state ($I_{hkl}(i)/I_{200T}(0)$, where $I_{hkl}(i)$ is the intensities of hkl reflections under an electric field of i kV mm^{-1}, and $I_{200T}(0)$ is the intensity of $\{200\}_T$ reflections at 0 kV mm^{-1}) as a function of the electrical loading. At the φ = 0° sector (Fig. 3a), the relative intensity of $\{200\}_T$ monotonically decreases upon increasing the electric field from −1.5 to 3 kV mm^{-1}, while the relative intensity of $\{002\}_T$ changes in the opposite direction. It should be noted that the intensity increase of $\{002\}_T$ and the intensity decrease of$\{200\}_T$ are similar between ±1.5 kV mm^{-1}, which means that the 90° domains equivalently switch between the directions parallel and perpendicular to the electric field when applying an electrical loading lower than $E_c/2$. Besides, the peak intensity for the monoclinic phase almost remains the same at the φ = 0° sector in the range of −1.5 to 3 kV mm^{-1}, implying that no phase transition has occurred under these conditions. In contrast, Fig. 3b shows that the relative intensity of $\{200\}_T$ at the φ = 90° sector remains constant in the range of −1.5 to 3 kV mm^{-1}, and the change of the $\{002\}_T$ peak intensity and the monoclinic phase intensity has an opposite tendency. It can thus be seen that anisotropic phase transition and domain switching occur in the polycrystalline ferroelectric ceramics. Furthermore, it is worth noting that the peak intensities at the $\{002\}_{PC}$ position exhibit tremendous changes between −1.5 and −2.5 kV mm^{-1}. This mutation would originate from the reconstruction of ferroelastic domains as discussed in the following sections.

Generally, once the displacement of domains is limited under the application of the electric field, the phase transformation would be enhanced and *vice versa*. As the sector verges on φ = 45°, the electric-field-driven phase transformation improves remarkably. Considering that no intergranular strain and preferred orientation induced by domain switching were detected at the φ = 45° sector, the structure refinement rather than peak fitting was employed for phase analysis in order to investigate the relationship between domain motion and phase transition and their contribution to the piezoelectric performance. For structure refinement, the monoclinic–tetragonal phase coexistence was employed as primitive structure models. To obtain steady refinements and minimize the number of variables, the coordinates of atoms of the monoclinic phase[8] were kept fixed for the applied bipolar electric field. Considering the existence of an electrostatic equilibrium between the external electric field, depolarization field, and average field over the volume of the crystal cell in dielectrics by applying an electric field, the polarization in every grain should be equal to macroscopic polarization. Furthermore, the flattening of the free energy profile near the MPB[26,27] would promote the spontaneous polarization in the monoclinic phase adapting to the tetragonal level at around 47 μC cm^{-2}(Table S1†). The well-refined structure results for 0.365BS–0.635PT at 2.5 kV mm^{-1} are shown in Fig. 4a. The detailed phase fraction is plotted in Fig. 4b. It shows that the phase transition occurs gradually in the range of −1.5 to 3 kV mm^{-1}, and the rate of linear phase transition is about 1.7%/[kV mm^{-1}], which is lower than that obtained from peak fitting on 0.36BS–0.64PT (4.2%/[kV mm^{-1}]).[10] This would originate from the difference between these two compounds in the phase construction. As the amplitude of the electric field is over ±4 kV mm^{-1}, the transformation rate increases up to about 3.6%/[kV mm^{-1}]. It should be noted that an electric field of transition “mutation” is prior to the coercive field. At around −1.5 and −2.5 kV mm^{-1}, the tetragonal phase rapidly transits to the monoclinic phase, and the transformation rate reaches up to 10.3%/[kV mm^{-1}]. Why does the phase transition rate vary suddenly at the electric field of −1.5 kV mm^{-1} rather than the E_c (−2.7 kV mm^{-1})? There should be an intrinsic correlation between the phase transition and domain switching/domain wall motion for compositions around the MPB as well, such that the texture intensity changes sharply accompanied by a phase transition as observed at the 0° sector. In view of the fact that the weak-field piezoelectric coefficient changes near the field of ±1.5 kV mm^{-1} (Fig. 1), unveiling the correlation of phase transition and domain switching would further elaborate the fundamental nature of the above-mentioned piezoelectric and ferroelectric performance.

The MPB ferroelectrics should be spatially heterogeneous systems due to the coexistence of multiphase and multidomain microstructures. To explain the role of phase coexistence and enhanced piezoelectricity around MPBs, it needs to be solved as a priority that what about the lattice-matching between ferroelectric phases and the mechanism of the phase transition between ferroelectric phases such as rhombohedral/monoclinic and tetragonal phases across the MPBs. It is well known that the total free energy in ferroelectrics includes bulk phase free energy, domain wall energy, and long-range electrostatic and elastostatic energies.[28] The lower free energy of the monoclinic phase near the MPB could be ascribed to the rotational polarization instabilities, and the appearance of monoclinic phase would dramatically decrease the domain wall energy.[29] To minimize the total free energy near the MPB, it is thus conceived that the tetragonal domains would be bridged by the monoclinic phase or domains. We propose the domain distribution around the MPB as the schematic diagram shown in Fig. 5. The existence of monoclinic bridging domains could lower the domain wall energy of the tetragonal phase caused by electrostatic and elastostatic functions.[29] The monoclinic bridging domains offer a low energy path for the transition of polarization between various polar axes in the tetragonal phase, and the rotational polarization in the monoclinic bridging domains makes the polarization vary continuously in MPB grains, facilitating the domain switching under external stimuli.

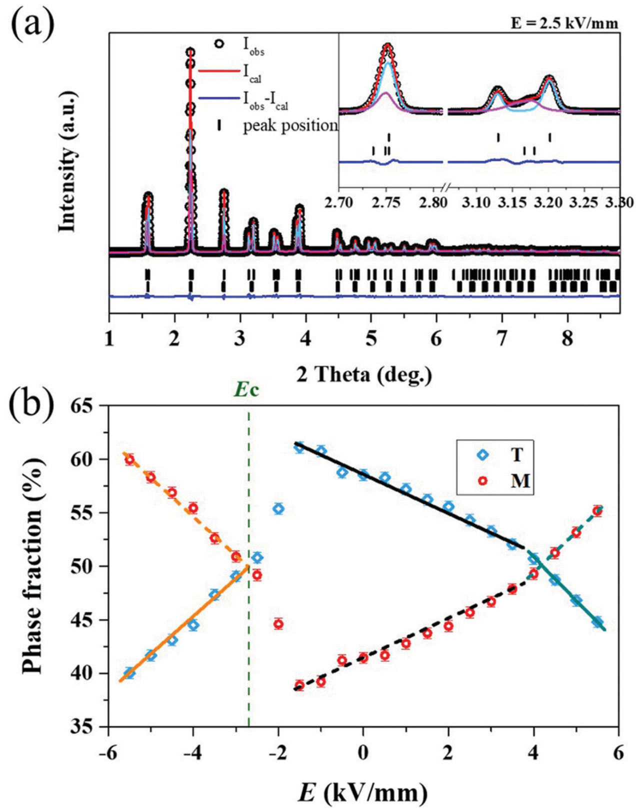

Fig. 4 (a) Structure refinement results of 0.365BS–0.635PT collected at 2.5 kV mm^{-1}. (b) Monoclinic–tetragonal phase fraction in 0.365BS–0.635PT when applying a bipolar electrical loading.

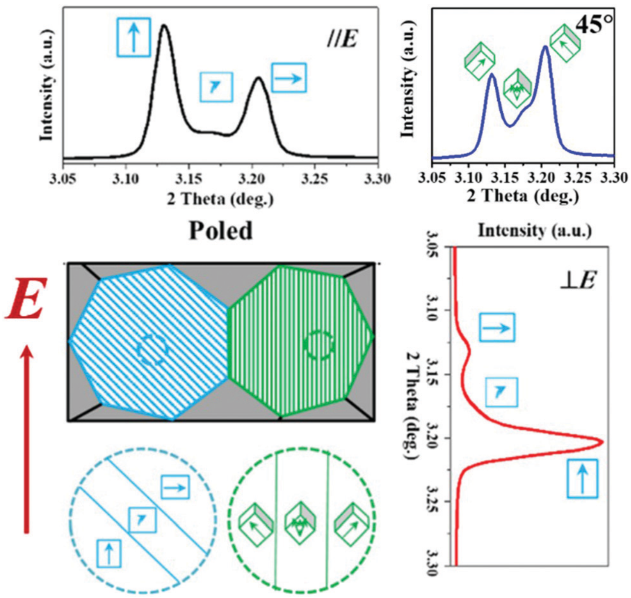

Fig. 5 The schematic diagram of the $\{002\}_{PC}$ diffraction profile of 90° domains in 001-oriented (cyan) and 101-oriented (green) grains. Herein, the 1-domain (↑) and 2-domain (→) correspond to the domains parallel and perpendicular to the electric field, respectively. The oblique arrow represents the monoclinic domains. In the 101-oriented grains, the polarization direction of the tetragonal phase makes a 45° angle with the electric field.

In Fig. 5, the diffraction profiles of domains from 001- and 101-oriented grains in poled 0.365BS–0.635PT are also plotted. Correspondingly, 1-domains marked as "↑" show stronger $(002)_T$ textured at the sector of 0° and $(200)_T$ textured at the sector of 90°. 2-domains are marked as "→", and their related $\{200\}_{PC}$ reflections are weaker than those of the 1-domains. These phenomena are in accord with the switching of domains parallel to the electric field. In the 101-oriented grains, the domains of the tetragonal phase compete to transfer to monoclinic domains rather than domain switching because their polarization direction makes a 45° angle with the electric field. Thus the intensity of $\{200\}_{PC}$ reflections of the tetragonal and monoclinic phases varies with a change in the electrical loading and they exhibit texture-free characteristics at the sector of 45°. To further account for the motion of domain walls in the present MPB polycrystalline ferroelectric, a series of schematic diagrams of domain distribution under the subcoercive field were proposed as shown in Fig. 6. Herein, a transition area was introduced in the schematic diagram. It is hypothesized that the domain wall motion and phase transition would occur initiatively at the transition area; according to the investigation results of the above-mentioned *in situ* diffraction, the intensity of $\{200\}_{PC}$ reflections of the monoclinic phase remains constant or changes linearly under the subcoercive field (−1.5 to −2.5 kV mm^{-1}). Besides, the domain wall and phase boundary would surmount a small potential barrier to move across the pinning at the transition area, and the d_{33} value increases rapidly at the weak field ($\alpha/d_{init} = 0.22 \times 10^{-6}$ m V^{-1}). Once the electrical loading exceeds $E_c/2$, the transition area would expand and the pinned tetragonal/monoclinic phase would start to transform into an alternative phase, and hence a high phase transition rate is observed. The destruction and reconstruction of the transition area would activate the pinned domains to promote their switching, resulting in enhanced piezoelectric performance. It is therefore concluded that the change in converse piezoelectric coefficients of 0.365BS–0.635PT below E_c is collectively contributed by the domain wall motion in the tetragonal phase and phase transition to the monoclinic phase. The existence and reconstruction of bridging monoclinic domains promote the switching of domains. Regulating the configuration of domains and the domain boundary would be further helpful in improving the ferroelectric and piezoelectric performance of MPB materials.

Conclusion

In summary, the Rayleigh model and *in situ* high-energy diffraction were used to study the nonlinear converse piezoelectric

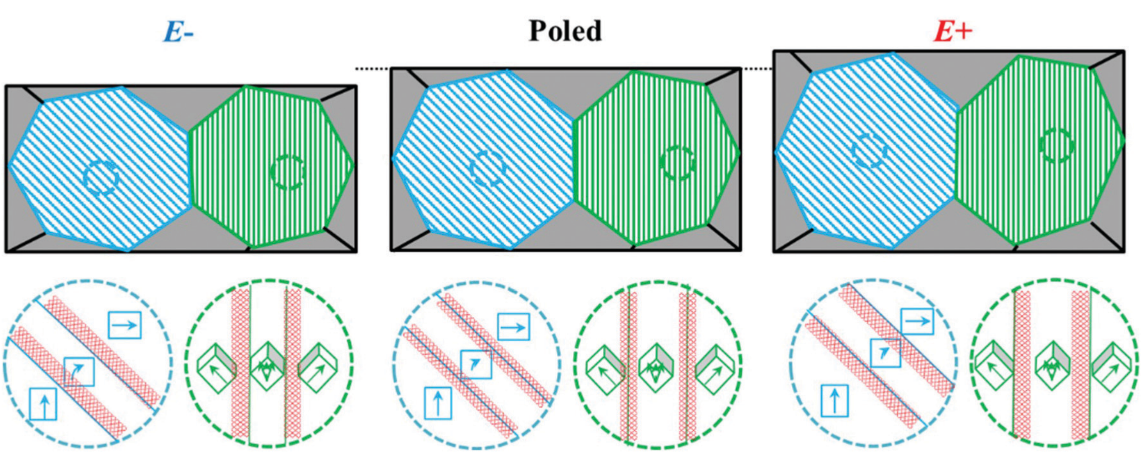

Fig. 6 The schematic diagram of domain switching in MPB ferroelectric polycrystals under a subcoercive field. The red zone between the monoclinic and tetragonal phases is defined as a transition area.

response in the MPB composition of $0.365BiScO_3$–$0.635PbTiO_3$ to investigate the role of phase coexistence in the domain wall motion. It is shown that the nonlinear response below the coercive field obeys the Rayleigh law. Using synchrotron-based X-ray diffraction, the evolution of domains and phase transformation have been evaluated. Both the change in Rayleigh variables and characteristic peak profiles imply that a phase transition occurs dramatically beyond the coercive field. Based on the present investigation, we constructed a configuration of the tetragonal domains bridged by the monoclinic phase or domains to explain the role of phase coexistence and enhanced piezoelectricity. It is speculated that the domain switching and phase transformation would take place firstly at a transition area between the tetragonal and monoclinic domains. The present investigation would provide an insight into the role of phase coexistence in enhancing the piezoelectric response and would be further beneficial for improving the ferroelectric and piezoelectric performance of MPB materials by controlling the configuration of domain walls.

Conflicts of interest

The authors declare that they have no known competing financial interests or personal relationships that could have appeared to influence the work reported in this paper.

Acknowledgements

This work was supported by the National Natural Science Foundation of China (Grants 21701126, 21801013, 21825102, 21731001, and 21590793) and the Fundamental Research Funds for the Central Universities, China (Grant FRF-TP-18-001C2). L. F. is thankful for the financial support from the China Scholarship Council and the help from Naike Shi. NSF's ChemMatCARS Sector 15 is principally supported by the Divisions of Chemistry (CHE) and Materials Research (DMR), National Science Foundation, under Grant No. NSF/CHE-1834750. The use of the Advanced Photon Source, an Office of Science User Facility operated for the U.S. Department of Energy (DOE) Office of Science by Argonne National Laboratory, was supported by the U.S. DOE under Contract No. DE-AC02-06CH11357.

References

1 Z. Chen, L. Hong, F. Wang, *et al.* Facilitation of ferroelectric switching via mechanical manipulation of hierarchical nanoscale domain structures, *Phys. Rev. Lett.*, 2017, **118**(1), 017601.

2 V. Nagarajan, A. Roytburd, A. Stanishevsky, *et al.* Dynamics of ferroelastic domains in ferroelectric thin films, *Nat. Mater.*, 2003, **2**(1), 43–47.

3 T. Tsuji, S. Saito, K. Fukuda, *et al.* Significant stiffness reduction at ferroelectric domain boundary evaluated by ultrasonic atomic force microscopy, *Appl. Phys. Lett.*, 2005, **87**(7), 071909.

4 A. K. Tagantsev, I. Stolichnov, E. L. Colla, *et al.* Polarization fatigue in ferroelectric films: Basic experimental findings, phenomenological scenarios, and microscopic features, *J. Appl. Phys.*, 2001, **90**(3), 1387–1402.

5 D. Damjanovic, A morphotropic phase boundary system based on polarization rotation and polarization extension, *Appl. Phys. Lett.*, 2010, **97**(6), 062906.

6 N. Huang, Z. Liu, Z. Wu, *et al.* Huge Enhancement of Electromechanical Responses in Compositionally Modulated Pb(Zr1-xTix)O3, *Phys. Rev. Lett.*, 2003, **91**(6), 067602.

7 L. Fan, J. Chen, Y. Ren, *et al.* Unique piezoelectric properties of the monoclinic phase in Pb(Zr,Ti)O3 ceramics: large lattice strain and negligible domain switching, *Phys. Rev. Lett.*, 2016, **116**(2), 027601.

8 M. Hinterstein, J. Rouquette, J. Haines, *et al.* Structural description of the macroscopic piezo-and ferroelectric properties of lead zirconate titanate, *Phys. Rev. Lett.*, 2011, **107**(7), 077602.

9 H. Liu, H. Huang, L. Fan, *et al.* Synergy between phase transformation and domain switching in two morphotropic phase boundary ferroelectrics, *Phys. Rev. Mater.*, 2018, **2**(11), 111403.

10 D. K. Khatua, C. M. Fancher, J. L. Jones, *et al.* Anomalous reduction in domain wall displacement at the morphotropic phase boundary of the piezoelectric alloy system PbTiO3-BiScO3, *Phys. Rev. B*, 2016, **93**(10), 104103.

11 H. Liu, J. Chen, H. Huang, *et al.* Role of reversible phase transformation for strong piezoelectric performance at the morphotropic phase boundary, *Phys. Rev. Lett.*, 2018, **120**(5), 055501.

12 T. Asada and Y. Koyama, Ferroelectric domain structures around the morphotropic phase boundary of the piezoelectric material PbZr1-xTixO3, *Phys. Rev. B: Condens. Matter Mater. Phys.*, 2007, **75**(21), 214111.

13 T. Hungría, F. Houdellier, M. Algueró, *et al.* Monoclinic symmetry of twin-free nanocrystals in the BiScO3-PbTiO3 solid solution as revealed by aberration-corrected TEM, *Phys. Rev. B: Condens. Matter Mater. Phys.*, 2010, **81**(10), 100102.

14 A. Pramanick, D. Damjanovic, J. E. Daniels, *et al.* Origins of electro–mechanical coupling in polycrystalline ferroelectrics during subcoercive electrical loading, *J. Am. Ceram. Soc.*, 2011, **94**(2), 293–309.

15 R. Eitel, C. A. Randall, T. R. Shrout and S.-E. Park, Preparation and characterization of high temperature perovskite ferroelectrics in the solid-solution (1-x)BiScO3-xPbTiO3, *Jpn. J. Appl. Phys., Part 1*, 2002, **41**, 2099.

16 B. Kim, P. Tong, D. Kwon, J. M. S. Park and B. G. Kim, Temperature-dependent neutron diffraction study of phase separation at morphotropic phase boundary in (1-x)BiScO3-xPbTiO3, *J. Appl. Phys.*, 2009, **105**, 114101.

17 D. K. Khatua, K. V. Lalitha, C. M. Fancher, J. L. Jones and R. Ranjan, Anomalous reduction in domain wall displace-

ment at the morphotropic phase boundary of the piezoelectric alloy system PbTiO3-BiScO3, *Phys. Rev. B*, 2016, **93**, 104103.

18 D. Damjanovic, Logarithmic frequency dependence of the piezoelectric effect due to pinning of ferroelectric-ferroelastic domain walls, *Phys. Rev. B: Condens. Matter Mater. Phys.*, 1997, **55**(2), R649.

19 D. Damjanovic and M. Demartin, The Rayleigh law in piezoelectric ceramics, *J. Phys. D: Appl. Phys.*, 1996, **29**(7), 2057.

20 G. Tutuncu, J. S. Forrester, J. Chen, *et al.* Extrinsic contributions to piezoelectric Rayleigh behavior in morphotropic PbTiO3-BiScO3, *Acta Mater.*, 2017, **137**, 45–53.

21 R. E. Eitel, T. R. Shrout and C. A. Randall, Nonlinear contributions to the dielectric permittivity and converse piezoelectric coefficient in piezoelectric ceramics, *J. Appl. Phys.*, 2006, **99**(12), 124110.

22 G. Tutuncu, D. Damjanovic, J. Chen, *et al.* Deaging and asymmetric energy landscapes in electrically biased ferroelectrics, *Phys. Rev. Lett.*, 2012, **108**(17), 177601.

23 L. Fan, L. Zhang, Y. Ren, *et al.* Relationship among the Crystal Structure, Texture, and Macroscopic Properties of Tetragonal (Pb,La)(Zr,Ti)O3 Ferroelectrics Investigated by In Situ High-Energy Synchrotron Diffraction, *Inorg. Chem.*, 2020, **59**(18), 13632–13638.

24 B. Kim, P. Tong, D. Kwon, *et al.* Temperature-dependent neutron diffraction study of phase separation at morphotropic phase boundary in (1-x)BiScO3-xPbTiO3, *J. Appl. Phys.*, 2009, **105**(11), 114101.

25 L. Fan, J. Chen, Y. Ren, *et al.* Structural correlation to piezoelectric and ferroelectric mechanisms in rhombohedral Pb (Zr,Ti)O3 ceramics by in-situ synchrotron diffraction, *Inorg. Chem.*, 2018, **57**(6), 3002–3007.

26 H. Fu and R. E. Cohen, Polarization Rotation Mechanism for Ultrahigh Electromechanical Response in Single-Crystal Piezoelectrics, *Nature*, 2000, **403**, 281–283.

27 D. Damjanovic, A morphotropic phase boundary system based on polarization rotation and polarization extension, *Appl. Phys. Lett.*, 2010, **97**(6), 062906.

28 W. F. Rao and Y. U. Wang, Bridging domain mechanism for phase coexistence in morphotropic phase boundary ferroelectrics, *Appl. Phys. Lett.*, 2007, **90**(18), 182906.

29 Y. M. Jin, Y. U. Wang, A. G. Khachaturyan, *et al.* Conformal miniaturization of domains with low domain-wall energy: Monoclinic ferroelectric states near the morphotropic phase boundaries, *Phys. Rev. Lett.*, 2003, **91**(19), 197601.